International Journal of Heat and Mass Transfer 69 (2014) 455–463

Contents lists available at ScienceDirect

International Journal of Heat and Mass Transfer

journal homepage: www.elsevier.com/locate/ijhmt

Simplification of pyrolytic reaction mechanism and turbulent heat transfer of n-decane at supercritical pressures

Bo Ruan [a], Hua Meng [a,*], Vigor Yang [b]

[a] School of Aeronautics and Astronautics, Zhejiang University, Hangzhou, Zhejiang 310027, China
[b] Daniel Guggenheim School of Aerospace Engineering, Georgia Institute of Technology, Atlanta, GA 30332, USA

ARTICLE INFO

Article history:
Received 30 April 2013
Received in revised form 2 September 2013
Accepted 20 October 2013

Keywords:
Convective heat transfer
Thermal decomposition
Supercritical pressure
Engine cooling
n-Decane

ABSTRACT

Fluid flows and heat transfer of hydrocarbon fuels with endothermic pyrolysis play an important role in regenerative cooling of many flight vehicles and energy-conversion devices. In this paper, an approach to simplifying the global pyrolytic reaction mechanism of n-decane is proposed for problems with mild endothermic pyrolysis at supercritical pressures. The basic idea lies in the fact that the high-molecular-weight alkane or alkene components in a thermally decomposed n-decane mixture possess similar thermophysical properties and make only minor contributions to heat absorption; they can thus be grouped together and represented by a single light species. Numerical tests indicate that a reduced 12-species reaction mechanism for mild cracking of n-decane represents a reasonable choice in terms of model accuracy and efficiency. The reduced pyrolytic reaction mechanism is employed to study the effect of mild thermal decomposition of n-decane on turbulent convective heat transfer at supercritical pressures. The wall heat flux can be increased significantly at high fluid temperatures, due mainly to heat absorption resulting from endothermic pyrolytic reactions.

1. Introduction

Fluid flows and heat transfer of hydrocarbon fuels at supercritical pressures play an important role in many regenerative cooling processes for aerospace and energy-conversion applications [1–4]. Because of the high heat load in liquid-propellant rocket and supersonic combustion ramjet (scramjet) engines, the combustion chamber wall generally requires active cooling to ensure engine reliability and durability. This can be accomplished by circulating engine fuel in the cooling channels surrounding high temperature regions. Since the operation pressure in the cooling channels is generally higher than the critical pressure of the hydrocarbon fuel, this leads to many peculiar fluid flow and heat transfer phenomena at supercritical pressures. One of the unique features of the processes lies in thermophysical property variations, which exert strong influences on fluid dynamics and heat transfer characteristics. The situation becomes even more distinct near the critical region, in which the fuel transits from a liquid-like to a gas-like state with drastic property variations [5].

In an active cooling process at a supercritical pressure, once the fuel temperature exceeds a threshold level, the fluid is thermally decomposed into variant components with low molecular weights, a phenomenon known as high-pressure pyrolysis. The pyrolytic reaction of a hydrocarbon fuel is typically endothermic. Therefore, in addition to heat absorption through sensible enthalpy variation, the pyrolytic process can enhance the heat-absorbing capacity through chemical energy changes of the fuel. This extra heat sink can contribute to the thermal management of flight vehicles and propulsion engines [6].

A variety of experimental studies have been carried out to elucidate high pressure pyrolytic reactions of hydrocarbon fuels. Song et al. [7] studied the pyrolysis of n-tetradecane at 450 °C over an elevated pressure range of 2–9 MPa, using a batch reactor. It was found that the major products in the early stage of the decomposition process are n-alkanes and 1-alkenes, while cyclic alkanes/alkenes and aromatics are formed in later stages. A general reaction mechanism was proposed to analyze the pyrolytic reactions. Thermal decomposition of C_{10}–C_{14} n-alkanes under near- and supercritical conditions were investigated by Yu and Eser [8], also using a batch reactor. A first-order reaction mechanism was developed to represent the pyrolytic kinetics, with the rate constants correlated to the carbon number of the hydrocarbon fuel. Stewart et al. [9] explored supercritical pyrolysis of decalin, tetralin, and n-decane at a temperature range of 700–810 K. The product distributions and probable reaction pathways were discussed. The caging effects commonly associated with liquid phase reactions were employed to explain the C_5 and C_6 ring contraction phenomenon. Ward et al. [10] investigated pressure effects on supercritical heat transfer of n-decane with mild thermal cracking. A one-step proportional product distribution (PPD) chemical model was proposed to predict fuel decomposition and product production.

* Corresponding author. Tel.: +86 571 87952990.
E-mail address: menghua@zju.edu.cn (H. Meng).

0017-9310/$ - see front matter © 2013 Elsevier Ltd. All rights reserved.
http://dx.doi.org/10.1016/j.ijheatmasstransfer.2013.10.045

Nomenclature

A	pre-exponential constant, s^{-1}
A_s	surface area, m^2
e_t	total energy, J kg^{-1}
E_a	activation energy, J mol^{-1}
h_i	enthalpy of a species i, J kg^{-1}
k_A	chemical reaction rate coefficient, s^{-1}
M_w	molecular weight, g mol^{-1}
p	pressure, Pa
q''	surface heat flux, W m^{-2}
Q'''	heat absorption rate per unit volume, W m^{-3}
R_u	universal gas constant, 8.314 J mol^{-1} K^{-1}
S	source term, kg m^{-3} s^{-1}
t	time, s
T	temperature, K
$\vec{u}$	velocity vector, m s^{-1}
Y	species mass fraction

Greeks

λ	thermal conductivity, W m^{-1} K^{-1}
ρ	density, kg m^{-3}
τ	viscous stress, N m^{-2}
$\dot{\omega}$	chemical reaction rate, mol s^{-1} m^{-3}

Subscripts

d	diffusion
endo	endothermic
i	species

Chakraborty and Kunzru [11] examined high-pressure pyrolysis of n-heptane, while Zhong et al. [12] conducted experimental studies of the thermal decomposition of aviation kerosene. Recently, DeWitt et al. [13] systematically examined the pyrolytic reactivity, product selectivity, and carbon deposition propensity of different aviation fuels under supercritical conditions.

A number of numerical studies have been performed to treat fluid flows and heat transfer of hydrocarbon fuels with endothermic pyrolysis at high pressures. Sheu et al. [14] considered thermal cracking and heat transfer of Norpar-13 under near- and super-critical conditions. The pyrolytic reaction kinetics was incorporated using a three-step global model, in which the product mixture was grouped into fuel, cracked liquids, and cracked gases. Results indicated that energy absorption through pyrolytic reactions produces important effects on the fuel and channel wall temperature. Goel and Boehman [15] developed a mathematical formulation to simulate jet fuel degradation in a heated pipe flow environment under high-pressure conditions. A global pyrolytic reaction model obtained from batch reactor studies was employed to study laminar fluid flows, heat transfer, and thermal decomposition in a circular tube. Six different fuels, including Norpar-13 and dodecane, were chosen for numerical calculations, with attention focused on bulk fuel temperature and uncracked fuel fractions at the tube outlet. Ward et al. [16] investigated fluid dynamics and heat transfer characteristics of n-decane with mild thermal cracking in a heated circular tube at high pressures. A one-step global reaction mechanism, known as the proportional product distribution (PPD) chemical model, was used to predict spatial variations of the fuel temperature and species mass fractions along the flow direction.

In this paper, a simplification of the pyrolytic reaction mechanism of n-decane is developed and implemented to efficiently study fluid flows and heat transfer at supercritical pressures. The work is based on the one-step proportional product distribution (PPD) chemical model developed by Ward et al. [10,16] for mild thermal cracking of n-decane. The present formulation accommodates a complete set of conservation equations of mass, momentum, energy, and species mass fractions. The research goal is to reduce the number of thermally cracked mixture components while still maintaining model accuracy. The effort leads to a reduced number of conservation equations of species mass fractions and decreased computational time for thermophysical property calculations. As a consequence, the numerical efficiency is considerably improved. The simplified pyrolytic reaction mechanism is then employed for a numerical study of flow dynamics and heat transfer characteristics of n-decane in a mini tube under a constant wall temperature. The effect of mild thermal decomposition on the heat transfer processes is carefully examined.

2. Theoretical formulation and model validation

In order to properly handle the chemically reacting flows and heat transfer processes under supercritical pressures, the following steady-state conservation equations are numerically solved:

Mass conservation:

$$\nabla \bullet (\rho \vec{u}) = 0 \tag{1}$$

Momentum conservation:

$$\nabla \bullet (\rho \vec{u}\vec{u}) = -\nabla p + \nabla \bullet \tau \tag{2}$$

Energy conservation:

$$\nabla \bullet (\rho \vec{u} e_t) = \nabla \bullet (\lambda \nabla T) - \nabla \bullet (p\vec{u}) \tag{3}$$

where the total energy, e_t, includes the energy of formation, and thus no extra source term from chemical reactions is needed.

Species conservation:

$$\nabla \bullet (\rho Y_i \vec{u}) = -\nabla \bullet (\rho Y_i \vec{u}_{d,i}) + S_i \tag{4}$$

where the source term resulting from the endothermic pyrolytic reaction can be expressed as

$$S_i = \dot{\omega}_i \bullet M_{wi} \tag{5}$$

In the present analysis, the baseline pyrolytic reaction kinetics for mild thermal cracking of n-decane is obtained from the one-step proportional product distribution (PPD) chemical model proposed by Ward et al. [10,16] based on their experimental measurements. In the PPD model, the measured mass fractions of the major decomposed products at different pressures were averaged to obtain a general reaction mechanism [10]. The model includes 18 species and was tested to be valid for mild thermal cracking of n-decane at a range of supercritical pressures between 3.45 and 11.38 MPa. The chemical reaction scheme has been reformulated in this work with full mass balance using the experimental data in [10,16] and is referred to as the 18-species mechanism in Table 1. The overall reaction is expressed as follows:

$$\begin{aligned} C_{10}H_{22} \rightarrow\ & 0.153CH_4 + 0.222C_2H_4 + 0.138C_2H_6 + 0.200C_3H_6 \\ & + 0.185C_3H_8 + 0.171C_4H_8 + 0.118C_4H_{10} \\ & + 0.149C_5H_{10} + 0.137C_5H_{12} + 0.170C_6H_{12} \\ & + 0.106C_6H_{14} + 0.147C_7H_{14} + 0.091C_7H_{16} \\ & + 0.132C_8H_{16} + 0.040C_8H_{18} + 0.046C_9H_{18} \\ & + 0.031C_9H_{20} \end{aligned} \tag{T1}$$

Table 1
n-Decane pyrolytic reaction mechanisms.

Coefficients of pyrolytic chemical reaction																	Number of species	Eq. No.
CH_4	C_2H_4	C_2H_6	C_3H_6	C_3H_8	C_4H_8	C_4H_{10}	C_5H_{10}	C_5H_{12}	C_6H_{12}	C_6H_{14}	C_7H_{14}	C_7H_{16}	C_8H_{16}	C_8H_{18}	C_9H_{18}	C_9H_{20}		
0.153	0.222	0.138	0.200	0.185	0.171	0.118	0.149	0.137	0.170	0.106	0.147	0.091	0.132	0.04	0.046	0.031	18	T1
0.153	0.222	0.138	0.200	0.185	0.171	0.118	0.149	0.137	0.170	0.106	0.371	0.162					14	T2
0.153	0.222	0.138	0.200	0.185	0.171	0.118	0.149	0.137	0.630	0.268							12	T3
0.153	0.222	0.138	0.200	0.185	0.171	0.118	0.958	0.405									10	T4

Based on this reaction kinetics, the pyrolytic reaction rate of n-decane with mild thermal cracking can be calculated as

$$\frac{d[C_{10}H_{22}]}{dt} = -k_A[C_{10}H_{22}] \tag{6}$$

where the rate constant is given as

$$k_A = A\exp(-E_a/R_uT) \tag{7}$$

The pre-exponential constant is $A = 1.6 \times 10^{15}\ s^{-1}$, and the activation energy is $E_a = 263.7$ kJ/mol [10]. In the following, this one-step reaction mechanism is further simplified by reducing the number of species components without sacrificing the model accuracy.

A key issue in the simulation of fluid flows and heat transfer at supercritical pressures is accurate estimation of thermophysical properties, which undergo strong variations with temperature, pressure, and mixture fractions, especially in the near-critical regime [5]. In our prior numerical studies, a general framework has been established for property evaluations. The Benedict–Webb–Rubin (BWR) equation of state for a reference fluid, propane, is used to calculate its density, with empirical expressions to determine viscosity and thermal conductivity [17]. Based on these reference properties, extended corresponding-state methods [18,19] are employed to calculate properties of a thermally decomposed supercritical mixture. Fundamental thermodynamic theories and the Soave–Redlich–Kwong (SRK) equation of state for the supercritical mixture are implemented to calculate other thermodynamic properties, such as heat capacity and internal energy [20]. An empirical correlation of Fuller [21] is used to calculate the binary mass diffusivity at low pressures, and a simple corresponding-state approach developed by Takahashi [22] is employed to take into account high-pressure effects. The overall methods for property evaluation have been successfully applied in previous numerical studies of supercritical-pressure heat transfer of cryogenic methane and n-heptane in mini tubes [3,4,23], supercritical droplet vaporization and dynamic responses to externally-imposed pressure oscillations [24–27], and cryogenic fluid injection, mixing, and combustion at supercritical conditions [28–30].

The aforementioned chemical kinetics and property evaluation methods have been implemented into a commercial CFD package, Fluent, through its user coding capability. A pressure-based numerical algorithm is employed to solve the conservation equations, along with user-developed functions for calculating thermophysical properties and chemical source terms in the species conservation equations. The $k-\varepsilon$ turbulent model with an enhanced wall treatment in Fluent [31], which solves a one-equation Wolfstein model in the near wall region if the meshes are within the viscous sublayer or applies a standard wall function if the meshes are not, is employed to achieve turbulence closure in the present study.

The numerical model has previously been used for studying supercritical heat transfer of hydrocarbon fuels without pyrolysis [3,4,23,32]. Since the species conservation equations and chemical source terms from the pyrolytic reaction of n-decane are incorporated herein, the model is further validated against the experimental and computational results of Ward et al. [10]. The numerical analysis is concerned with fluid flows and heat transfer of n-decane with mild endothermic pyrolysis in a mini tube, as shown schematically in Fig. 1. Variations of the fluid mixture density, thermal conductivity, bulk temperature, axial velocity, and conversion rate of n-decane are shown in Fig. 2. Excellent agreement with existing data is obtained under various operating conditions.

3. Results and discussion

3.1. Pyrolytic reaction mechanism reduction

The theoretical and numerical framework developed in the early section is first employed to facilitate the reduction of the PPD pyrolytic reaction scheme proposed by Ward et al. for n-decane [10,16]. The basic idea lies in the fact that the mildly cracked products, with relatively high molecular weights, such as alkanes and alkenes, make only minor contributions to the heat absorbing process. Furthermore, they possess similar thermophysical properties and can thus be grouped together and represented by a single light component, C_7H_{16} for alkanes and C_7H_{14} for alkenes in the C_7, C_8, and C_9 groups, respectively. In the reduced reaction scheme, Eq. (T2), the mole fractions of C_7H_{16} and C_7H_{14} are increased, while the mole fractions of all other species remain the same as in Eq. (T1). As a consequence, a simplified one-step global reaction can be established with fewer mixture components. This approach is similar to finding surrogate models for practical fuels. The following equation represents the reduced mechanism involving 14 species. The stoichiometric coefficients are listed in Table 1.

$$\begin{aligned} C_{10}H_{22} \rightarrow\ & 0.153CH_4 + 0.222C_2H_4 + 0.138C_2H_6 + 0.200C_3H_6 \\ & + 0.185C_3H_8 + 0.171C_4H_8 + 0.118C_4H_{10} \\ & + 0.149C_5H_{10} + 0.137C_5H_{12} + 0.170C_6H_{12} \\ & + 0.106C_6H_{14} + 0.371C_7H_{14} + 0.162C_7H_{16} \end{aligned} \tag{T2}$$

The global reaction scheme presented by Eq. (T2) can be further reduced by grouping the high-molecular-weight alkanes and alkenes together and representing them with a single light alkane and alkene species, respectively. This leads to the 12- and 10-species mechanisms, as given below in Eqs. (T3) and (T4). The stoichiometric coefficients are also listed in Table 1.

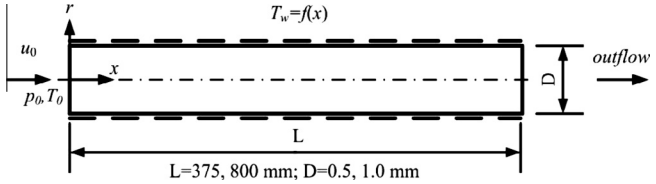

Fig. 1. Schematic configuration.

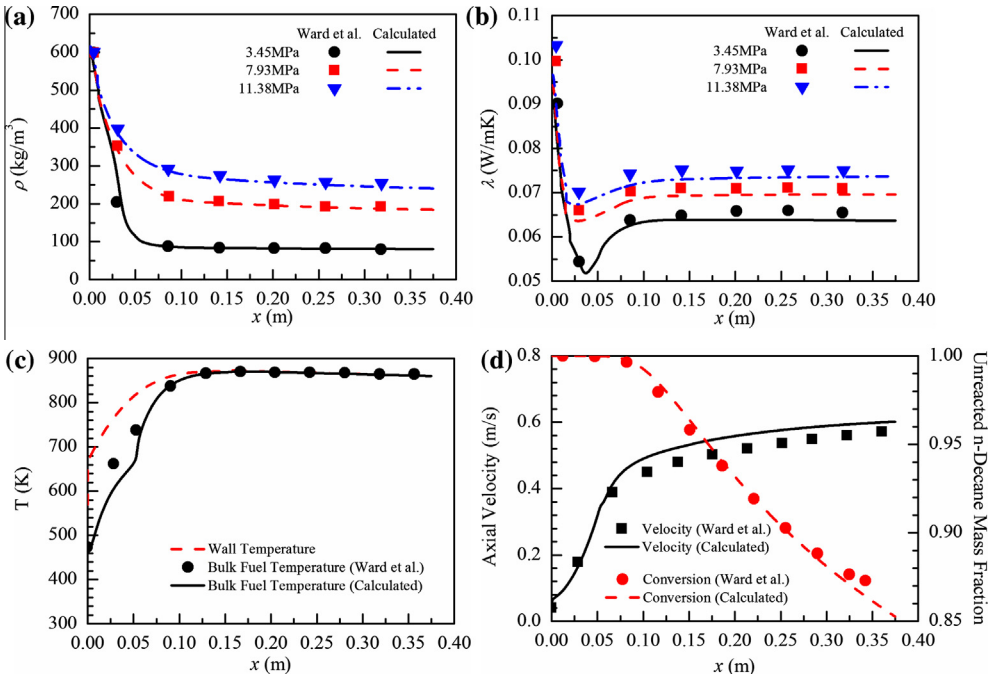

Fig. 2. Model validation; (a) density, (b) thermal conductivity, (c) bulk fluid temperature at 3.45 MPa, (d) axial velocity and n-decane conversion rate at 3.45 MPa (data for comparisons are from Ref. [10]).

$$C_{10}H_{22} \rightarrow 0.153CH_4 + 0.222C_2H_4 + 0.138C_2H_6 + 0.200C_3H_6 + 0.185C_3H_8 + 0.171C_4H_8 + 0.118C_4H_{10} + 0.149C_5H_{10} + 0.137C_5H_{12} + 0.630C_6H_{12} + 0.268C_6H_{14} \quad (T3)$$

$$C_{10}H_{22} \rightarrow 0.153CH_4 + 0.222C_2H_4 + 0.138C_2H_6 + 0.200C_3H_6 + 0.185C_3H_8 + 0.171C_4H_8 + 0.118C_4H_{10} + 0.958C_5H_{10} + 0.405C_5H_{12} \quad (T4)$$

The accuracy of the simplified mechanisms in the prediction of fluid dynamics and heat transfer characteristics of n-decane with mild endothermic pyrolytic reactions at supercritical pressures will next be fully investigated. The research goal is to develop a reduced global chemical reaction scheme with high fidelity to improve numerical efficiency while maintaining model accuracy.

The model validation effort follows the experiments of Ward et al. [10,16] over various operating pressures, wall temperatures, and inlet mass fluxes. As shown in Fig. 1, the physical configuration is concerned with supercritical fluid flows and heat transfer of n-decane with mild endothermic pyrolysis in a mini tube. The tube diameter is 0.5 mm and measures a length of 375 mm [10]. The experimentally-measured wall temperature is prescribed in the numerical studies. Because of the geometric and physical symmetry in the configuration, the present numerical calculations are simplified to be axisymmetric.

A grid independence study was first conducted. Three different sets of grid points, 55 × 5000, 80 × 5000, and 55 × 8000 in the radial and axial directions, were tested. Fig. 3 shows the calculated fluid velocities and the conversion rates of n-decane at the tube axis for the three different meshes. Negligible differences among the results were observed. The smallest grid system, 55 × 5000, was thus chosen for the present numerical study.

Different reduced reaction mechanisms were tested at a supercritical pressure of 3.45 MPa. The critical pressure and temperature of n-decane are 2.12 MPa and 617.7 K, respectively. The distribution of the tube wall temperature with a maximum value at 873 K is specified based on experimental data [10], as shown in Fig. 2c. The inlet volumetric flow rate is 0.5 ml/min. Fig. 4 shows the calculated axial velocity, n-decane conversion rate, and bulk fluid temperature, along with the measurements of Ward et al. [10]. The axial velocity increases as the fuel cracks to form low-molecular-weight species, and the fluid density decreases. The difference between the results of the baseline and reduced 10-species mechanisms appears to be quite small, with a maximum relative error around 4% in this case (see Fig. 4a). Fig. 4b shows the n-decane conversion rates calculated from different reaction mechanisms. The discrepancies between various chemical schemes are modest. The maximum relative difference between the baseline and 10-species mechanisms is 0.6%. A similar observation is made for the bulk fluid temperature.

Fig. 5 shows the distributions of the calculated thermophysical properties using different endothermic reaction mechanisms. The fluid density decreases as the cracked high-molecular-weight components are grouped and replaced, and the thermal conductivity increases. The maximum relative difference in the calculated fluid density is around 3.8% between the 18- and 10-species mechanisms, and only 1% in thermal conductivity. The fluid

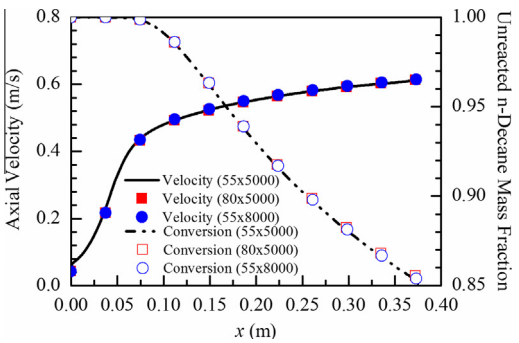

Fig. 3. Results from grid-independence studies.

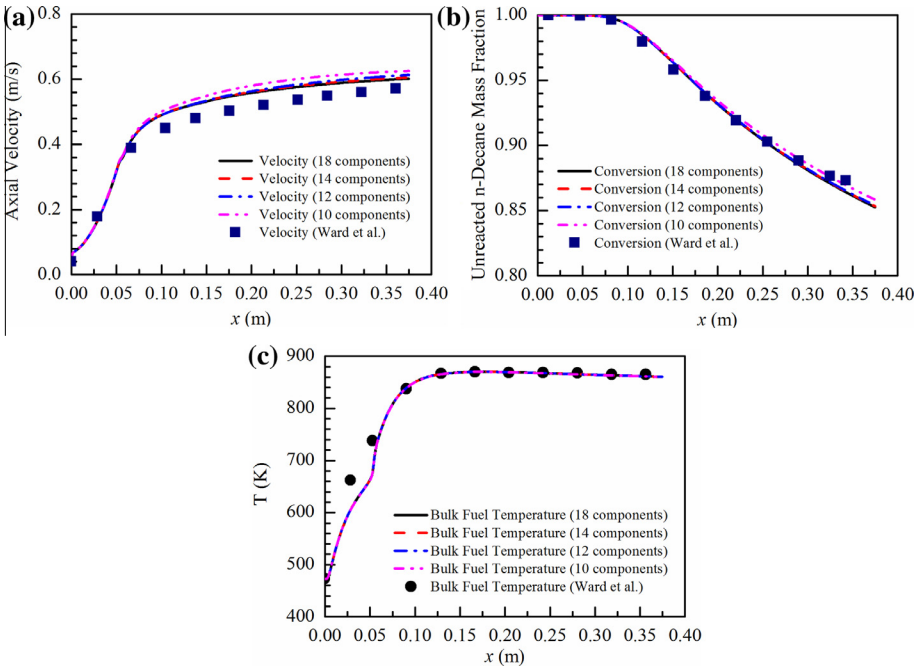

Fig. 4. Numerical results from different reaction mechanisms at 3.45 MPa; (a) axial velocity, (b) n-decane conversion rate, (c) bulk fluid temperature.

density variation is consistent with the velocity evolution shown in Fig. 4b. Fig. 5c shows the heat capacity; the relative difference in the results from the various reaction mechanisms is negligibly small.

Based on the numerical results discussed above, a simplified n-decane pyrolytic reaction mechanism involving 10 species, which reduces eight cracked products through component grouping, appears to be a reasonable choice in terms of model simplicity and accuracy. The largest relative differences for all the calculated results between the baseline and reduced reaction mechanisms are within 5%, with the maximum appearing in the axial velocity, as shown in Fig. 4a.

The effect of pressure on the simplified reaction mechanisms is next investigated. Figs. 6 and 7 show the distributions of the axial velocity and n-decane conversion rate at 7.93 and 11.38 MPa. The relative differences between the 18- and 10-species mechanisms are around 6.8% and 7.4%, respectively. Because the relative errors both increase to more than 5%, the 10-species reaction mechanism is considered inaccurate at these two supercritical pressures. The 12-species mechanism is thus tested. The relative differences in

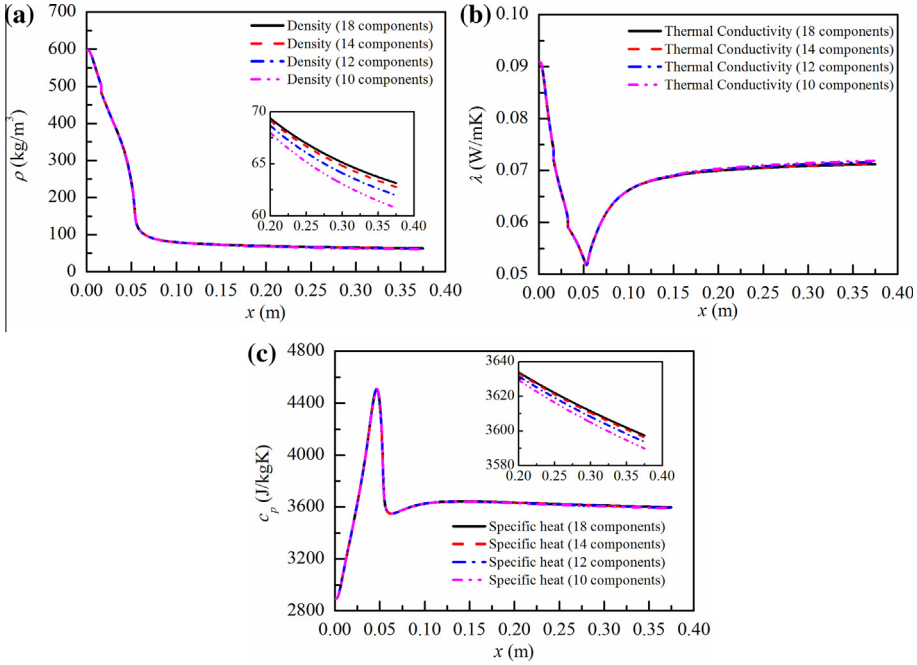

Fig. 5. Thermophyscial properties of cracked supercritical mixture calculated using different reaction mechanisms at 3.45 MPa; (a) density, (b) thermal conductivity, (c) constant-pressure heat capacity.

the axial velocity between the 18- and 12-species mechanisms are both around 3% at the two pressures. The relative difference of the n-decane conversion rate is only 1.3% at 7.93 MPa and 2.8% at 11.38 MPa. Based on the test results at three different supercritical pressures, as shown in Figs. 4–7, the 12-species reduced global reaction mechanism is determined to be a good choice.

Since the axial velocity exhibits the largest relative error calculated using different reaction mechanisms, special attention is paid to this variable in conducting further numerical tests concerning the effect of the inlet mass flow rate on the reaction mechanism reduction. In the following study, the maximum wall temperature is changed to 823 K, consistent with the experimental conditions [10]. The operating pressure is set to 7.93 MPa. Fig. 8 shows the distributions of the axial velocity based on three different reaction mechanisms. Two different inlet volumetric flow rates of 0.3 and 0.7 ml/min are considered. It should be mentioned that the inlet volumetric flow rate in Fig. 6 is 0.5 ml/min. The largest relative difference from the 18- and 12-species reaction mechanisms is around 2%, occurring at an inlet flow rate of 0.3 ml/min, as shown in Fig. 8a. For comparison, the largest relative error for the 10-species reaction mechanism is around 4% at the same low inlet flow rate. This is attributed to the fact that at a low inlet flow rate, more fuel is thermally decomposed because of the increased fluid temperature. The effect of the reaction mechanism on fluid flow and heat transfer thus increases, but it is still minor, with mild thermal decomposition, as shown in Fig. 8a.

Based on the results discussed above, it is concluded that the 12-species reaction mechanism reduced from the baseline 18-species PPD chemical model [10,16] is a good choice for numerical simulations of fluid flows and heat transfer of n-decane with mild endothermic pyrolysis at supercritical pressures. The largest relative differences are less than 5% for all the flow and thermophysical properties. This 12-species reduced reaction mechanism is obtained by separately grouping the cracked C_6, C_7, C_8, and C_9 alkanes and alkenes and representing them using a single light component, with C_6H_{14} for the alkanes and C_6H_{12} for the alkenes.

A main reason for simplifying the PPD pyrolytic reaction mechanism is to improve the model efficiency for simulations of fluid flows and heat transfer. Table 2 gives the computational time in the present supercritical heat transfer simulations. All the calculations were performed using a 40-core Downing PHPC100 workstation. The simulation based on the baseline 18-species

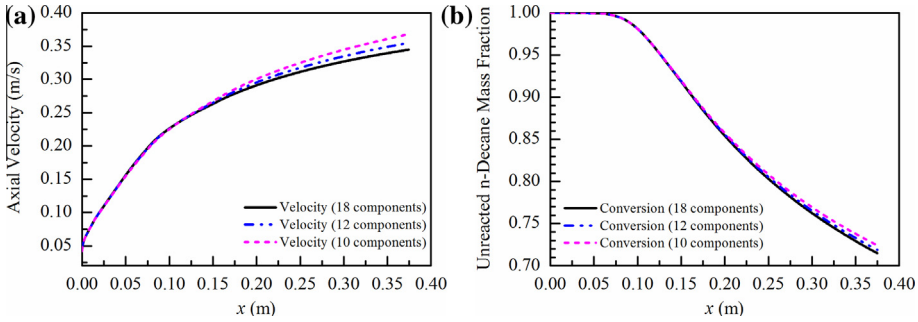

Fig. 6. Numerical results from different reaction mechanisms at 7.93 MPa; (a) axial velocity, (b) n-decane conversion rate.

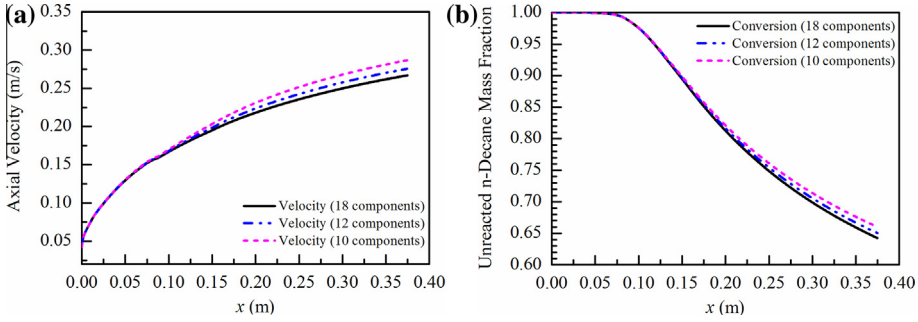

Fig. 7. Numerical results from different reaction mechanisms at 11.38 MPa; (a) axial velocity, (b) n-decane conversion rate.

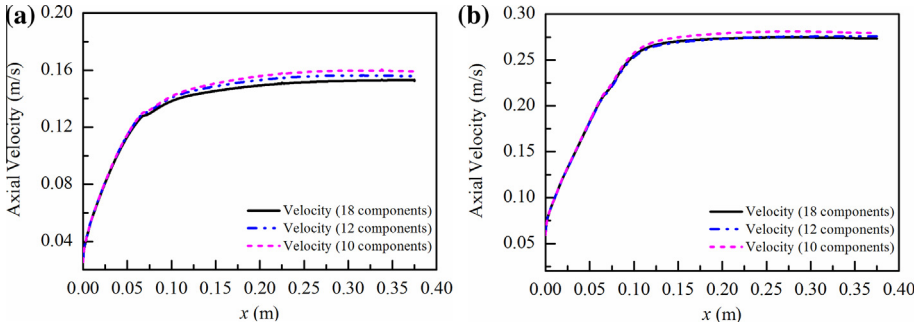

Fig. 8. Axial velocity calculated using different reaction mechanisms at different inlet mass flow rates; (a) 0.3 ml/min, (b) 0.7 ml/min.

reaction mechanism required approximately 2500 iterations and 66 h to converge, while the computational time were decreased to around 24 h using the reduced 12-species reaction mechanism. This represents a 63% improvement in computational efficiency. The computational time was further decreased to 17 h with the 10-species reaction mechanism, but the model accuracy was worsened slightly, as the relative error exceeded 5% for several cases. It should be noted that the number of computational iterations to convergence varies slightly for the different reaction mechanisms, but the effect on computational time is minor. The iteration number is intentionally kept the same in the present studies for clear comparisons.

The significant improvement in numerical efficiency using simplified reaction mechanisms is related to the reduction in the species conservation equations and thermophysical property calculations. In the present study, they each account for about one half of the savings in computational time.

3.2. Heat transfer study

To further demonstrate its robustness, the reduced 12-species global reaction mechanism was applied to simulate turbulent fluid flows and heat transfer of n-decane with mild thermal decomposition in a mini tube, as shown schematically in Fig. 1. The tube diameter is 1 mm, and its length is 800 mm. To ensure a fully developed flow before heat transfer starts, an inlet section with 150 mm in length is thermally insulated. An outlet section with 150 mm in length is also thermally insulated to minimize the effect of outflow boundary conditions on numerical results. The 500 mm long middle section is heated, with a constant wall temperature of 1000 K. Based on the results of a more thorough grid-independence study, a computational mesh of 50×5600 in the radial and axial directions, respectively, was chosen for the present numerical simulations.

The study focuses on the effect of endothermic pyrolytic reactions on the flow dynamics and heat transfer characteristics. The inlet pressure is set at 6 MPa, well above the critical pressure of n-decane (2.12 MPa). The inlet flow velocity varies from 0.5 to 2.0 m/s to ensure mild thermal decomposition of n-decane. The operating conditions are detailed in Table 3.

Fig. 9 shows the distributions of the fluid temperature at the tube axis under conditions with and without pyrolysis. The inlet flow velocity is 1.0 m/s. The effect of endothermic decomposition appears approximately from $x/D = 300$, at which point the thermal cracking of n-decane starts to speed up, as shown in Fig. 10. At the end of the heated section ($x/D = 500$), the fluid temperature with pyrolysis is 22 K lower than that without pyrolysis. The temperature difference between the two cases appears to be modest for two reasons: mild thermal cracking of n-decane (i.e., less than 20% of decomposition, as shown in Fig. 10), and increased wall heat flux at a fixed constant wall temperature in the case with pyrolysis.

To elucidate the second point, the wall heat-flux distributions for the two cases are examined, as shown in Fig. 11. With pyrolysis, the wall heat flux increases from $x/D = 300$ and eventually leads to more than 280% increase of the wall heat flux at the end of the heated section. Compared with the case without pyrolysis, heat absorption by thermal decomposition significantly influences the heat transfer process at high fluid temperatures. Therefore, under the condition of a constant wall temperature, it is more appropriate to compare wall heat flux rather than fluid temperature in the analysis of the effect of endothermic pyrolytic reactions on heat transfer characteristics.

Fig. 10 also shows the distributions of the flow velocity under conditions with and without pyrolysis. With pyrolytic reactions, the flow velocity at the thermal exit exceeds 11 m/s, while it is only around 8 m/s for the case without pyrolysis. Such a difference can be attributed to the change of fluid density in the heat transfer process. Fig. 12 shows that the fluid density decreases with increasing temperature. Once the thermal decomposition occurs, as shown in

Table 2
Computational times using different reaction mechanisms.

Equation number	Number of species	Iterations	Computational times/(hour)
T1	18	2500	65.7
T3	12	2500	24.4
T4	10	2500	16.7

Table 3
Operating conditions for numerical studies.

Parameters	Values
Inlet pressure, p_0	6 MPa
Wall temperature, T_w	1000 K
Inlet temperature, T_0	300 K
Inlet velocity, u_0	0.5–2.0 m/s

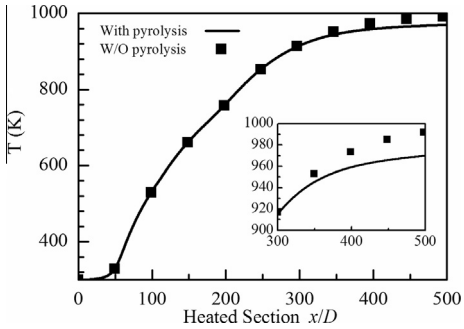

Fig. 9. Fluid temperature distributions at tube axis with and without pyrolysis.

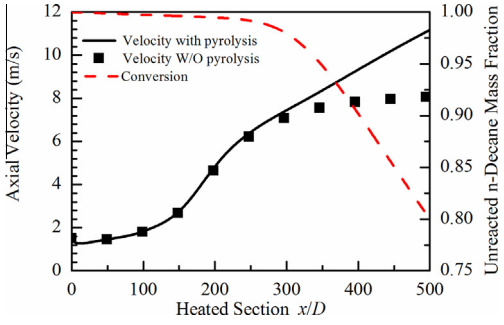

Fig. 10. Distributions of flow velocity and n-decane mass fraction at tube axis.

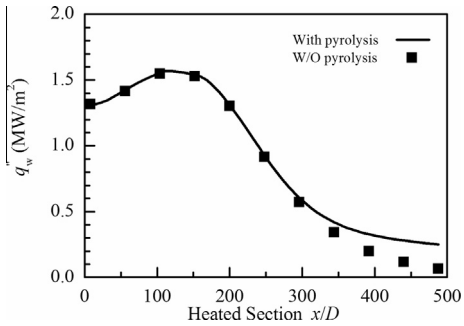

Fig. 11. Distributions of total wall heat flux with and without pyrolysis.

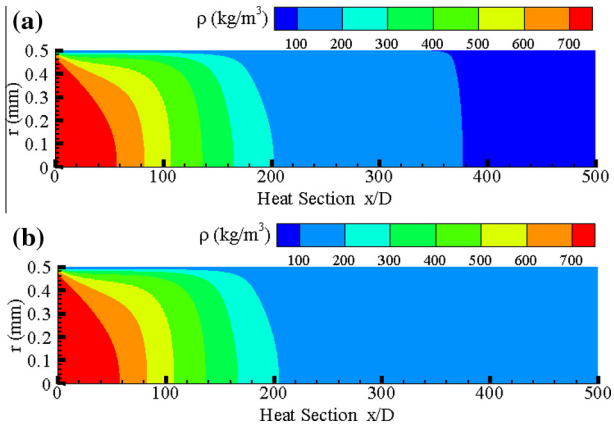

Fig. 12. Fluid density distributions; (a) with pyrolysis, (b) without pyrolysis.

Fig. 12a, the formation of low-molecular-weight components further decreases the density of the fluid mixture by around 28% (starting from $x/D = 380$), leading to a corresponding increase of the flow velocity.

The effect of the inlet flow velocity on the convective heat transfer of n-decane with endothermic pyrolytic reactions is also investigated in the range of 0.5–2.0 m/s, with all the other operating parameters remaining unchanged, as summarized in Table 3. To quantify the heat absorption by endothermic pyrolytic reactions, a wall heat flux resulting from endothermic chemical reactions is defined as

$$q''_{endo} = \frac{\int_{\Delta V} Q'''_{endo} dV}{\Delta A_s} \tag{8}$$

where A_s is the surface area of the tube wall, and Q'''_{endo} the endothermic heat absorption rate per unit volume, defined as,

$$Q'''_{endo} = \Sigma_i S_i h_i \tag{9}$$

The enthalpy, h_i, includes both the enthalpy of formation and sensible enthalpy.

Fig. 13 shows the distributions of the wall heat flux from endothermic reactions with three different inlet velocities. The heat flux first increases rapidly, due to the rise of fluid temperature, which enhances thermal decomposition reactions, as indicated by Eq. (7). The wall heat flux then levels off and even decreases slowly, due to the decrease of n-decane mass fraction, which weakens the pyrolytic reactions, as indicated by Eq. (6). Fig. 13 shows that for the inlet flow velocity of 2.0 m/s, the wall heat flux resulting from endothermic chemical reactions reaches its highest value at the thermal exit. This phenomenon can be attributed to the relatively high fluid density and n-decane mass fraction, as shown in Fig. 14.

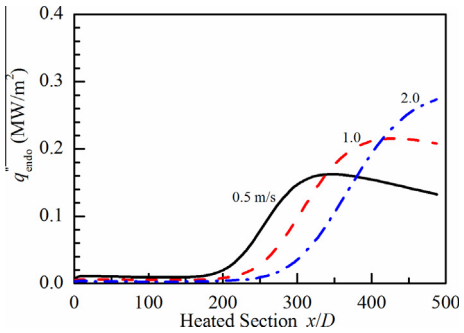

Fig. 13. Distributions of surface heat flux from endothermic reaction at three inlet velocities.

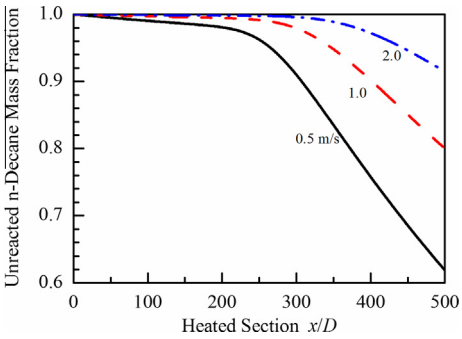

Fig. 14. Distributions of n-decane mass fraction at three inlet velocities.

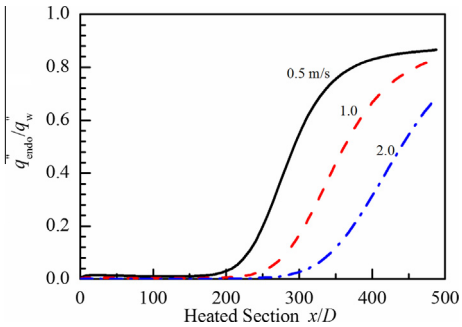

Fig. 15. Distributions of ratio between surface heat flux from endothermic reaction and total wall heat flux from convective heat transfer at three inlet velocities.

Fig. 15 shows the comparison between the wall heat fluxes from endothermic chemical reactions and the total wall heat fluxes from convective heat transfer at three different inlet flow velocities. At a low inlet flow velocity of 0.5 m/s, the heat flux ratio is above 0.8 near the thermal exit, clearly indicating that a significant portion of the total wall heat flux is contributed by heat absorption from endothermic pyrolytic reactions. The heat flux ratio decreases as the inlet flow velocity increases, but still exceeds 0.6 at the thermal exit with an inlet velocity of 2.0 m/s. The heat absorption resulting from endothermic pyrolytic reactions dictates the convective heat transfer process at high fluid temperatures. The situation is more profound with a low inlet flow velocity and consequently a weak convective heat transfer process.

4. Conclusions

Fluid flows and heat transfer of hydrocarbon fuels at supercritical pressures play an important role in regenerative cooling processes for many propulsion and power-generation systems. In this paper, an approach to simplifying the global n-decane pyrolytic reaction mechanism has been developed to improve the efficiency of numerical simulations of fluid flows and heat transfer with mild endothermic pyrolysis. The formulation is based on a complete set of conservation equations of mass, momentum, energy, and species mass fractions. Thermophysical properties of cracked n-decane supercritical mixtures are accurately calculated. A baseline global n-decane pyrolytic reaction mechanism from the PPD model containing 18 alkane and alkene species is considered. Since the high-molecular-weight alkane or alkene components in the cracked n-decane mixture possess similar thermophysical properties and make only minor contributions to heat absorption, they can be separately grouped together and represented by a

single light alkane or alkene species. This reduction approach is similar to finding surrogate ingredients for commercial fuels.

The reduction approach for prolytic reaction mechanisms has been numerically verified for chemically reacting flows and heat transfer of n-decane in a circular tube under various operating conditions at supercritical pressures. Results indicate that a reduced 12-species reaction mechanism appears to be a good choice in terms of computational efficiency and accuracy. The largest relative difference between the 12-species and the baseline 18-sepcies mechanisms is within 5%, but the computational time can be decreased by more than 60%. This improvement is achieved mainly through reduced conservation equations of species mass fractions and decreased computational time for thermophysical property calculations. Each factor contributes approximately half of the improvement in numerical efficiency.

The reduced 12-species pyrolytic reaction mechanism is employed for numerical studies of turbulent heat transfer of n-decane in a mini tube with an isothermal wall. The effect of thermal decomposition and ensuing heat absorption are investigated at a supercritical pressure of 6 MPa. Results show that the wall heat flux is increased significantly at high fluid temperatures, due to the n-decane endothermic pyrolysis, which contribute to more than 60% of the total wall heat flux from convective heat transfer under test conditions. The heat absorption resulting from thermal decomposition thus dictates the convective heat transfer process at high fluid temperatures.

Acknowledgments

This research was financially supported by the Zhejiang Provincial Natural Science Foundation of China (R1100300) and the William R.T. Oaks Endowment of the Georgia Institute of Technology.

References

[1] D.R. Sobel, L.J. Spadaccini, Hydrocarbon fuel cooling technologies for advanced propulsion, J. Eng. Gas Turbines Power 119 (1997) 344–351.
[2] M. Pizzarelli, F. Nasuti, R. Paciorri, M. Onofri, Numerical analysis of three-dimensional flow of supercritical fluid in asymmetrically heated channels, AIAA J. 47 (2009) 2534–2543.
[3] Y.-X. Hua, Y.-Z. Wang, H. Meng, A numerical study of supercritical forced convective heat transfer of n-heptane inside a horizontal miniature tube, J. Supercrit. Fluids 52 (2010) 36–46.
[4] Y.-Z. Wang, Y.-X. Hua, H. Meng, Numerical study of supercritical turbulent convective heat transfer of cryogenic-propellant methane, J. Thermophys. Heat Transfer 24 (2010) 490–500.
[5] V. Yang, Modeling of supercritical vaporization, mixing, and combustion processes in liquid-fueled propulsion systems, Proc. Combust. Inst. 28 (2001) 925–942.
[6] T. Edwards, Cracking and deposition behavior of supercritical hydrocarbon aviation fuels, Combust. Sci. Technol. 178 (2006) 307–334.
[7] C. Song, W.-C. Lai, H.H. Schobert, Condensed-phase pyrolysis of n-tetradecane at elevated pressures for long duration. Product distribution and reaction mechanisms, Ind. Eng. Chem. Res. 33 (1994) 534–547.
[8] J. Yu, S. Eser, Thermal decomposition of C10–C14 normal alkanes in near-critical and supercritical regions: product distributions and reaction mechanisms, Ind. Eng. Chem. Res. 36 (1997) 574–584.
[9] J. Stewart, K. Brezinsky, I. Glassman, Supercritical pyrolysis of decalin, tetralin, and n-decane at 700–800 K. Product distribution and reaction mechanism, Combust. Sci. Technol. 136 (1998) 373–390.
[10] T.A. Ward, J.S. Ervin, S. Zabarnick, L. Shafer, Pressure effects on flowing mildly-cracked n-decane, J. Propul. Power 21 (2005) 344–355.
[11] J.P. Chakraborty, D. Kunzru, High pressure pyrolysis of n-heptane, J. Anal. Appl. Pyrol. 86 (2009) 44–52.
[12] F.Q. Zhong, X.J. Fan, G. Yu, J. Li, Thermal cracking of aviation kerosene for scramjet applications, Sci. China Ser. E: Technol. Sci. 52 (2009) 2644–2652.
[13] M.J. DeWitt, T. Edwards, L. Shafer, D. Brooks, R. Striebich, S.P. Bagley, M.J. Wornet, Effect of aviation fuel type on pyrolytic reactivity and deposition propensity under supercritical conditions, Ind. Eng. Chem. Res. 50 (2011) 10434–10451.
[14] J.-C. Sheu, N. Zhou, A. Krishnan, Thermal cracking of norpar-13 under near-critical and supercritical conditions, AIAA Paper 1998-3758, 1998.
[15] P. Goel, A.L. Boehman, Numerical simulation of jet fuel degradation in flow reactors, Energy Fuels 14 (2000) 953–962.
[16] T.A. Ward, J.S. Ervin, R.C. Striebich, S. Zabarnick, Simulations of flowing mildly-cracked normal alkanes incorporating proportional product distributions, J. Propul. Power 20 (2004) 394–402.
[17] B.A. Younglove, J.F. Ely, Thermophysical properties of fluids II. Methane, ethane, propane, isobutane, and normal butane, J. Phys. Chem. Ref. Data 16 (1987) 577–796.
[18] J.F. Ely, H.J.M. Hanley, Prediction of transport properties. 1. Viscosity of fluids and mixtures, Ind. Eng. Chem. Fundam. 20 (1981) 323–332.
[19] J.F. Ely, H.J.M. Hanley, Prediction of transport properties. 2. Thermal conductivity of pure fluids and mixtures, Ind. Eng. Chem. Fundam. 22 (1983) 90–97.
[20] H. Meng, V. Yang, A unified treatment of general fluid thermodynamics and its application to a preconditioning scheme, J. Comput. Phys. 189 (2003) 277–304.
[21] R.C. Reid, J.M. Prausnitz, B.E. Poling, The Properties of Gases and Liquids, 4th ed., McGraw-Hill, 1987.
[22] S. Takahashi, Preparation of a generalized chart for the diffusion coefficients of gases at high pressures, J. Chem. Eng. (Japan) 7 (1974) 417–420.
[23] B. Ruan, H. Meng, Supercritical heat transfer of cryogenic-propellant methane in rectangular engine cooling channels, J. Thermophys. Heat Transfer 26 (2012) 313–321.
[24] H. Meng, G.C. Hsiao, V. Yang, J.S. Shuen, Transport and dynamics of liquid oxygen droplets in supercritical hydrogen streams, J. Fluid Mech. 527 (2005) 115–139.
[25] P. Lafon, H. Meng, V. Yang, M. Habiballah, Vaporization of liquid oxygen (LOX) droplets in hydrogen and water environments under sub- and super-critical conditions, Combust. Sci. Technol. 180 (2008) 1–26.
[26] G.C. Hsiao, H. Meng, V. Yang, Pressure-coupled vaporization response of n-pentane fuel droplet at subcritical and supercritical conditions, Proc. Combust. Inst. 33 (2011) 1997–2003.
[27] H. Meng, V. Yang, Clustering effects of liquid oxygen (LOX) droplet vaporization in hydrogen environments at subcritical and supercritical pressures, Int. J. Hydrogen Energy 37 (2012) 11815–11823.
[28] N. Zong, H. Meng, S.Y. Hsieh, V. Yang, A numerical study of cryogenic fluid injection and mixing under supercritical conditions, Phys. Fluids 16 (2004) 4248–4261.
[29] Y. Yin, X. Lu, Effects of injection temperature on the jet evolution under supercritical conditions, Chin. Sci. Bull. 54 (2009) 4197–4204.
[30] N. Zong, V. Yang, Near-field flow and flame dynamics of LOX/methane shear-coaxial injector under supercritical conditions, Proc. Combust. Inst. 31 (2007) 2309–2317.
[31] Fluent 6.3 User Guide, Fluent Inc., Lebanon, New Hampshire, USA, 2006.
[32] L. Wang, Z. Chen, H. Meng, Numerical study of conjugate heat transfer of cryogenic methane in rectangular engine cooling channels at supercritical pressures, Appl. Therm. Eng. 54 (2013) 237–246.